Available online at www.sciencedirect.com
ScienceDirect
Journal of Power Sources 174 (2007) 779–783
JOURNAL OF POWER SOURCES
www.elsevier.com/locate/jpowsour

Short communication

Computer simulation of a porous positive electrode for lithium batteries

Takayuki Doi [a], Hirotaka Fukudome [b], Shigeto Okada [a], Jun-Ichi Yamaki [a,*]

[a] *Institute for Materials Chemistry and Engineering, Kyushu University, 6-1 Kasuga-koen, Kasuga 816-8580, Japan*
[b] *Interdisciplinary Graduate School of Engineering Sciences, Kyushu University, 6-1 Kasuga-koen, Kasuga 816-8580, Japan*

Available online 27 June 2007

Abstract

The discharge characteristics of a Li/Li_yCoO_2 cell were simulated by numerical calculations. Based on the program proposed by Newman's group, the change in entropy due to lithium-ion insertion into the active materials was introduced into the open-circuit potential (OCP) for more practical applications. The OCP of $LiCoO_2$ ($y = 1$) at a full-discharge state was 3.82 V, which was determined from the original program. However, it should show a rapid decrease to minus infinity when discharge is complete ($y = 1$), which is due to the introduced entropy term. In addition, the local use of active materials across the Li_yCoO_2 electrode was not uniform, whereas the original program showed a constant value throughout the electrode. Based on the present results, the introduction of an entropy term to the OCP of Li_yCoO_2 works reasonably well for more practical applications.

Keywords: Lithium-ion batteries; Positive electrode; Computer simulation; Change in entropy; Rate capability

1. Introduction

Rechargeable lithium-ion batteries have been used in a wide variety of portable electric devices due to their high energy densities. However, these batteries still need to be improved before they can be used in hybrid electric vehicles (HEV) [1,2]. Rapid charge and discharge reactions are required when lithium-ion batteries are used for high power applications. Thus, lithium-ion transfer must be very rapid in such batteries. Lithium-ion transfer in lithium batteries consists of four different steps; lithium-ion diffusion through positive electrode materials, lithium-ion transport through an electrolyte, and lithium-ion transfer across the interfaces between the electrolyte and active electrode materials. Of these steps, the diffusion of lithium-ion through active electrode materials is well known to be slow. In addition, the charge transfer resistance at the electrode/electrolyte interface is expected to be low by extending the effective surface area of the active materials. Therefore, fine particles of battery active materials (ca. 5–10 μm) are used to reduce the diffusion path in commercial lithium-ion batteries [3–5]. In lithium-ion batteries intended for high power use, the particle sizes of active materials still need to be reduced further [6]. We previously prepared nano-sized $LiCoO_2$ particles by an excess lithium method or by laser ablation, and reported that the rate performance was improved by use of the resultant nano-sized $LiCoO_2$ compared with that using micron-sized $LiCoO_2$ powder [7,8]. However, the cell performance was influenced not only by the particle size of the active materials, but also by other geometric factors such as the thickness of the electrode. Such inherent complications should be mainly due to the porous structure of the electrodes; the ohmic potential drop and mass transfer were very intricate, and there was no way to separate them. Some powerful methods are needed to review the experimental results methodically, which should contribute to the design of high-power batteries. It may be useful to simulate cell performance by calculation. Doyle et al. proposed a mathematical model of a Li/insertion electrode cell using a porous electrode theory, and reported the simulation results [9,10]. Newman et al. studied the charge/discharge characteristics of a dual-insertion cell of $C/LiMn_2O_4$ by numerical calculation, and compared them with experimental data [11,12].

In the present study, the discharge characteristics of a Li/Li_yCoO_2 cell were studied by numerical calculation using the program proposed by Newman et al. [13]. Based on that program, we introduced changes in entropy to the OCP for more practical applications.

2. Model development

The program used (dual. f (version 4.0)) is freely available from Newman's group through their website. The program is

* Corresponding author. Tel.: +81 92 583 7790; fax: +81 92 583 7790.
E-mail address: yamaki@cm.kyushu-u.ac.jp (J.-I. Yamaki).

0378-7753/$ – see front matter © 2007 Elsevier B.V. All rights reserved.
doi:10.1016/j.jpowsour.2007.06.089

based on a cell model consisting of a porous positive-electrode, a separator, and a lithium metal negative-electrode. The porous electrode was composed of sphere-shaped particles of active materials, inert conductive additives, and polymer binder. The void space in the electrode was filled with an electrolyte solution. In the model, the one-dimensional transport of lithium-ion from the negative electrode to the positive electrode through the separator was considered, and the electrochemical insertion of lithium-ion was assumed to occur at all points on the active materials. The program was composed of six differential equations, which are described elsewhere in detail [11,13]:

(1) material balance on the electrolyte;
(2) current flow through the electrolyte;
(3) current flow through the active materials;
(4) pore-wall flux subjected to the Butler–Volmer equation, which is related to the divergence of the current flow in the electrolyte;
(5) Fick's first law for spherical diffusion;
(6) Fick's second law for spherical diffusion.

These equations were solved simultaneously to obtain the following solutions:

(1) lithium-ion concentration in the electrolyte,
(2) lithium-ion potential in the electrolyte,
(3) lithium-ion concentration on the active material particles,
(4) ionic current flowing through the electrolyte,
(5) pore-wall flux across the interface between the active materials and electrolyte,
(6) surface potential of the active materials.

In the present work, $LiCoO_2$ was used as the active material for the porous positive-electrode. Accordingly, the overall reaction can be described as follows:

$$Li_yCoO_2 + (1-y)Li \rightleftarrows LiCoO_2$$

The cell model is shown schematically in Fig. 1. The thickness of the negative electrode, the separator, and the positive electrode were set to 100, 25, and 100 μm, respectively. The surface of the negative electrode was defined as $x = 0$. The diffusion coefficient of lithium-ion within $LiCoO_2$ particles and a standard rate constant (k^0) were determined based on the literature [14]. The former was assumed to be constant at $1.0 \times 10^{-16}\ m^2\ s^{-1}$. The latter was evaluated to be $1.5 \times 10^{-6}\ A\ mol^{-3/2}\ m^{9/2}$ from the value for charge transfer resistance (R_{ct}) (Eq. (1)):

$$R_{ct} = \frac{RT}{Fj_0} \tag{1}$$

where R is a gas constant, T the absolute temperature, and F is the Faraday constant.

In this study, the effects of particle size of $LiCoO_2$, porosity in the porous positive-electrode, and conductivity of the positive electrode on the cell performance were investigated. Hence, the preset parameters in the original program were used except for those mentioned above. The change in the electrode potential of the Li_yCoO_2 electrode with lithium content (y), which was obtained from the original program, is shown with a broken line in Fig. 2. The OCP decreased from 4.7 V toward 3.8 V with an increase in y, but never fell below 3.82 V. In addition, the electrode potential varied linearly at around $y = 1$ with an increase in y, whereas a rapid decrease in electrode potential is seen in a real cell [15]. The Butler–Volmer equation (Eq. (2)) used in the program was

$$j = j_0 \left\{ \exp\left[\frac{0.5F(\eta - U)}{RT}\right] - \exp\left[\frac{-0.5F(\eta - U)}{RT}\right] \right\} \tag{2}$$

where j is the current density, η is an overpotential defined as $\eta = \Phi_1 - \Phi_2$ (Φ_1, Φ_2: electrical potential on the active material surface and in the electrolyte, respectively), and U is the OCP. An exchange current density of j_0 is defined as

$$j_0 = Fk^0 C^{0.5} (C_{smax} - C_{ss})^{0.5} C_{ss}^{0.5} \tag{3}$$

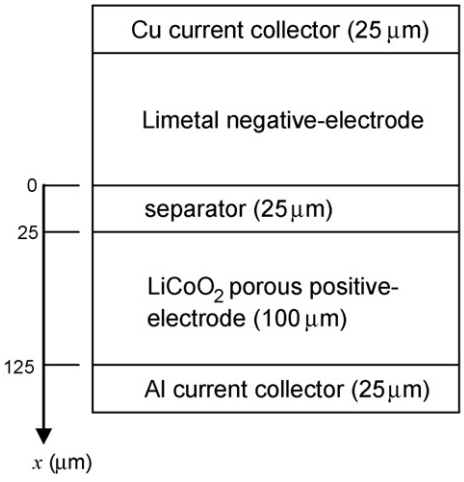

Fig. 1. A schematic model of a lithium battery.

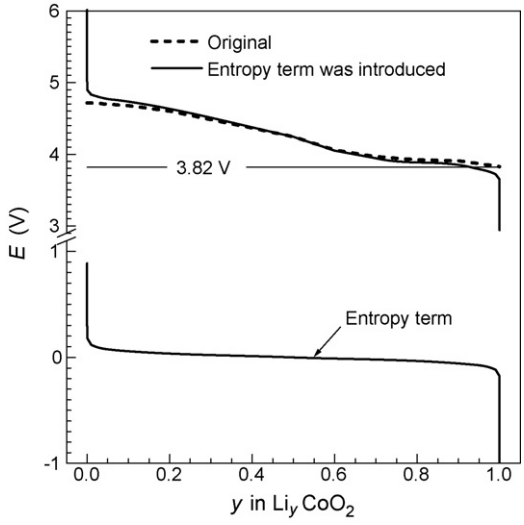

Fig. 2. Variation of the open-circuit potential of the Li_yCoO_2 electrode before and after changes in entropy were introduced into the OCP of Li_yCoO_2. Particle size of Li_yCoO_2: 100 nm, conductivity of the positive electrode: 100 S m^{-1}, porosity in the positive electrode: 0.772.

where C_{smax} is the maximum concentration of lithium-ion in $LiCoO_2$ ($y = 1$), C_{ss} is the lithium-ion concentration on the surface of $LiCoO_2$ particles, and C is the lithium-ion concentration in the electrolyte. In the present work, the change in entropy due to lithium-ion insertion into the active materials was introduced to U as follows [16,17]; as a first order approximation, interactions among Li-ions in Li_yCoO_2 were ignored:

$$U' = U - \frac{RT}{F} \ln \left[\frac{y}{1-y} \right] \quad (4)$$

U' was then substituted for U in Eq. (2).

3. Results and discussion

The change in the OCP with y after introduction of the entropy term is shown with a solid line in Fig. 2. The electrode potential showed a rapid decrease at around $y = 1$ and fell below 3.82 V, which is very similar to the results obtained with a real cell [15]. The entropy term also varied rapidly at around $y = 1$, as shown in Fig. 2. These results indicate that the OCP curves were affected by the variation of entropy with y.

Fig. 3a shows the variation in discharge capacity (broken line) with current density, as obtained with the original program. Cell voltage, positive-electrode and negative-electrode potentials at the end of discharge are also shown with solid line in Fig. 3a. The cell voltage was defined as the difference between the electrode potentials. The particle size of $LiCoO_2$, conductivity of the positive electrode, and porosity in the positive electrode were set to 100 nm, 100 S m^{-1}, and 0.772, respectively. The positive-electrode potential at the end of discharge fell to only 3.82 V even at a low current density of 1.0 mA cm^{-2}, and remained above 3.5 V at current densities of less than 15 mA cm^{-2}. On the other hand, the negative-electrode potentials increased with an increase in the current density, which should be due to overpotentials. As a result, the cell voltage never reached 3.5 V at current densities of less than 15 mA cm^{-2}. Fig. 3b shows the variation in discharge capacity, cell voltage, positive-electrode and negative-electrode potentials with current density that was obtained with the program after the entropy term was introduced into U. Even at a low current density of 1.0 mA cm^{-2}, the positive-electrode potential dropped to 3.49 V at the end of discharge and the cell voltage fell to 3.5 V. Although the potentials of both electrodes increased with an increase in the current density, the cell voltage still dropped to 3.5 V at the end of discharge regardless of the value of the current density; since discharge was cut off at a potential difference of 3.5 V and the negative-electrode potential increased with increasing current density, the positive-electrode potentials at the end of discharge increased with an increase in the current density, as shown in Fig. 3b. A discharge capacity of 137 mAh g^{-1} was obtained at 1.0 mA cm^{-2}, and gradually decreased to 130 mAh g^{-1} at 15 mA cm^{-2} followed by a significant decrease at current densities above 20 mA cm^{-2}.

Fig. 4 shows the use of active material in the Li_yCoO_2 electrode at the end of discharge. The original program gave a constant value of $y = 1.0$ throughout the entire electrode (broken line). On the other hand, the introduction of the entropy term

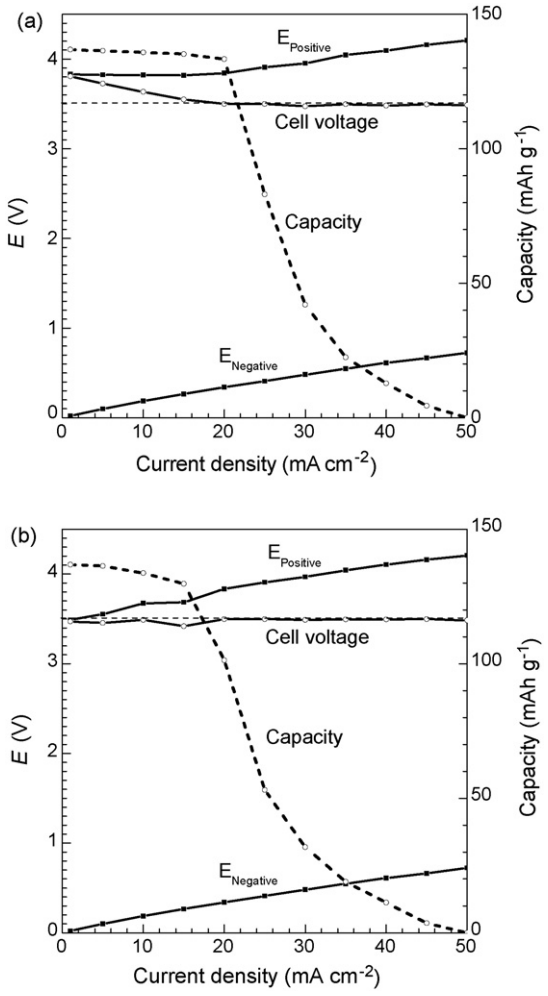

Fig. 3. Variation of discharge capacity and the cell voltage at the end of discharge with current density (a) before and (b) after variation of entropies was introduced into the OCP of Li_yCoO_2. Particle size of Li_yCoO_2: 100 nm, conductivity of the positive electrode: 100 S m^{-1}, volume fraction of electrolyte in the positive electrode: 0.772.

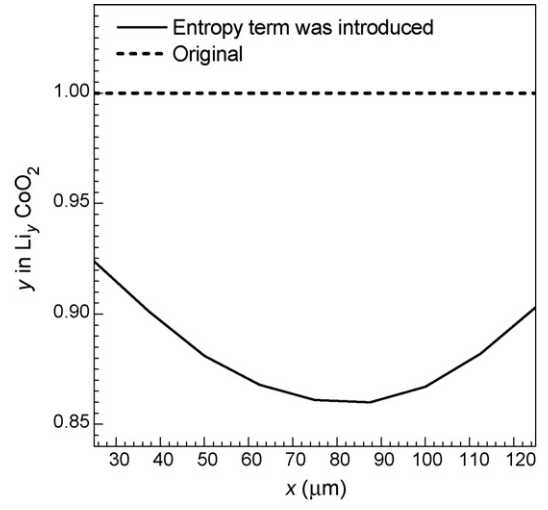

Fig. 4. Local use of active material in the Li_yCoO_2 electrode at the end of the discharge reaction. Particle size of Li_yCoO_2: 100 nm, conductivity of the positive electrode: 100 S m^{-1}, porosity in the positive electrode: 0.772.

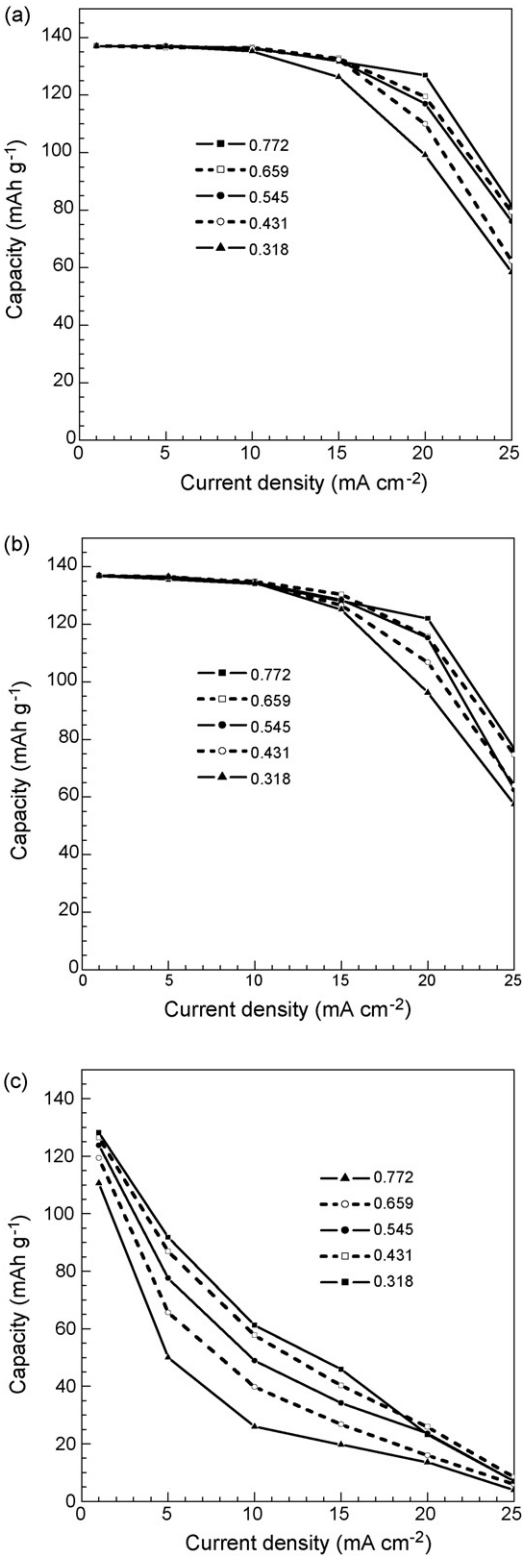

Fig. 5. Changes in discharge capacity with current density at various porosities in the positive electrode (ranging from 0.318 to 0.772). The particle size of Li_yCoO_2 was (a) 10 nm, (b) 100 nm, and (c) 1 μm. Conductivity of the positive electrode was 1.00 S m^{-1}.

resulted in a difference in y across the electrode (solid line); y gave a smaller value of 0.87 in the middle of the electrode than at both ends of the electrode, which should be due to the influence of ionic and electric conductivity. These results provide evidence that the introduced entropy should work reasonably well in the program to affect cell performance. These results indicate that the introduction of an entropy term into U' makes it possible to control the discharge reaction within a range of predetermined voltages.

The influence of porosity in the positive electrode on cell performance was investigated by using the program that included an entropy term. Fig. 5 shows the variation in discharge capacity with current density at various porosity values ranging from 0.318 to 0.772. The particle sizes of $LiCoO_2$ used in Fig. 5(a)–(c) were 10 nm, 100 nm, and 1 μm, respectively. The discharge capacity tended to increase with a decrease in particle size. The porosity at which a maximum capacity could be obtained differed depending on the particle size of $LiCoO_2$; the particle size of 10 nm gave the largest capacities when the porosity was 0.545, and the corresponding values were 0.431 and 0.318 for 100 nm and 1 μm, respectively. These results suggest that there should be an optimal value for the porosity of a porous electrode to enhance the rate performance of batteries.

4. Conclusion

Based on the program proposed by Newman's group, the discharge characteristics of a Li/Li_yCoO_2 cell were simulated by numerical calculations. Changes in entropy during the insertion of lithium-ion were introduced into the OCP, and their effects on the discharge characteristics were studied. The discharge voltage fell to 3.5 V, and a rapid decrease in the electrode potential was seen at around $y = 1$ with an increase in y by introducing the entropy term, which are similar to the results obtained in a real cell. In addition, nonuniformity in the local use of active materials across the Li_yCoO_2 electrode was observed. These results indicate that the entropy term we introduced should work reasonably well for more practical applications. The discharge performance was investigated using $LiCoO_2$ particles of various sizes, ranging from 10 nm to 1 μm. The porosity that gave the largest capacity was different depending on the particle size of the active materials.

Acknowledgement

The present work was supported by CREST of JST (Japan Science and Technology Agency).

References

[1] M. Winter, J.O. Besenhard, M.E. Spahr, P. Novák, Adv. Mater. 10 (1998) 725.
[2] Z. Ogumi, M. Inaba, Bull. Chem. Soc. Jpn. 71 (1998) 521.
[3] M.D. Levi, D. Aurbach, J. Phys. Chem. B 101 (1997) 4641.
[4] Z. Ogumi, T. Abe, T. Fukutsuka, S. Yamate, Y. Iriyama, J. Power Sources 27 (2004) 72.
[5] J. Barker, R. Pynenburg, R. Koksbang, M.Y. Saidi, Electrochim. Acta 41 (1996) 2481.

[6] T. Doi, Y. Iriyama, T. Abe, Z. Ogumi, Chem. Mater. 17 (2005) 1580.
[7] T. Kawamura, M. Makidera, S. Okada, K. Koga, N. Miura, J. Yamaki, J. Power Sources 146 (2005) 27.
[8] T. Tsuji, T. Kakita, T. Hamagami, T. Kawamura, J. Yamaki, M. Tsuji, Chem. Lett. 33 (2004) 1136.
[9] M. Doyle, T.F. Fuller, J. Newman, J. Electrochem. Soc. 140 (1993) 1526.
[10] M. Doyle, J. Newman, J. Appl. Electrochem. 27 (1997) 846.
[11] T.F. Fuller, M. Doyle, J. Newman, J. Electrochem. Soc. 141 (1994) 1.
[12] P. Arora, M. Doyle, A.S. Gozdz, R.E. White, J. Newman, J. Power Sources 88 (2000) 219.
[13] J. Newman, K.E. Thomas-Alyea, Electrochemical Systems, 3rd ed., Wiley–Interscience, 2004.
[14] Y.H. Rho, K. Kanamura, J. Electrochem. Soc. 151 (2004) A1406.
[15] J.N. Reimers, J.R. Dahn, J. Electrochem. Soc. 139 (1992) 2091.
[16] J. Yamaki, M. Egashira, S. Okada, J. Power Sources 90 (2000) 116.
[17] J. Yamaki, M. Makidera, T. Kawamura, M. Egashira, S. Okada, J. Power Sources 153 (2006) 245.